





Liposomal AntagomiR-155-5p Restores Anti-Inflammatory Macrophages and Improves Arthritis in Preclinical Models of Rheumatoid Arthritis

Audrey Paoletti,¹  Bineta Ly,¹ Catherine Cailleau,² Fan Gao,³ Marie Péan de Ponfilly-Sotier,¹ Juliette Pascaud,¹ Elodie Rivière,¹ Luxin Yang,⁴ Lilian Nwosu,⁴ Aziza Elmesmari,⁴ Franceline Reynaud,² Magali Hita,² David Paterson,³ Julien Reboud,³ Francois Fay,² Gaetane Nocturne,^{1,5}  Nicolas Tsapis,² Iain B. McInnes,⁴  Mariola Kurowska-Stolarska,⁴ Elias Fattal,² and Xavier Mariette^{1,5} 

Objective. We previously reported an increased expression of microRNA-155 (miR-155) in the blood monocytes of patients with rheumatoid arthritis (RA) that could be responsible for impaired monocyte polarization to anti-inflammatory M2-like macrophages. In this study, we employed two preclinical models of RA, collagen-induced arthritis and K/BxN serum transfer arthritis, to examine the therapeutic potential of antagomiR-155-5p entrapped within PEGylated (polyethylene glycol [PEG]) liposomes in resolution of arthritis and repolarization of monocytes towards the anti-inflammatory M2 phenotype.

Methods. AntagomiR-155-5p or antagomiR-control were encapsulated in PEG liposomes of 100 nm in size and –10 mV in zeta potential with high antagomiR loading efficiency (above 80%). Mice were injected intravenously with 1.5 nmol/100 µL PEG liposomes containing antagomiR-155-5p or control after the induction of arthritis.

Results. We demonstrated the biodistribution of fluorescently tagged PEG liposomes to inflamed joints one hour after the injection of fluorescently tagged PEG liposomes, as well as the liver's subsequent accumulation after 48 hours, indicative of hepatic clearance, in mice with arthritis. The injection of PEG liposomes containing antagomiR-155-5p decreased arthritis score and paw swelling compared with PEG liposomes containing antagomiR-control or the systemic delivery of free antagomiR-155-5p. Moreover, treatment with PEG liposomes containing antagomiR-155-5p led to the restoration of bone marrow monocyte defects in anti-inflammatory macrophage differentiation without any significant functional change in other immune cells, including splenic B and T cells.

Conclusion. The injection of antagomiR-155-5p encapsulated in PEG liposomes allows the delivery of small RNA to monocytes and macrophages and reduces joint inflammation in murine models of RA, providing a promising strategy in human disease.

INTRODUCTION

Monocytes and macrophages are key players in the pathogenesis and therapeutic response in rheumatoid arthritis (RA).^{1–5} A number of studies have found an increase of pro-inflammatory

macrophage recruitment and activation in synovium in both human and mouse models.^{4,6–8} On the other hand, the overexpression of some microRNAs (miRs) associated with inflammation has been detected in the blood and synovium of patients with RA. Among these miRs, an up-regulation of miR-155 expression

Supported by the Foundation for Research in Rheumatology (project 045).

¹Audrey Paoletti, PhD, Bineta Ly, IE, Marie Péan de Ponfilly-Sotier, MD, Juliette Pascaud, IE, Elodie Rivière, MD, PhD, Gaetane Nocturne, MD, PhD, Xavier Mariette MD, PhD: Paris-Saclay University, INSERM UMR1184, Center for Immunology of Viral Infections and Autoimmune Diseases, Le Kremlin Bicêtre, France; ²Catherine Cailleau, IE, Franceline Reynaud, PhD, Magali Hita, MSc, Francois Fay, PhD, Nicolas Tsapis, PhD, Elias Fattal, PharmD, PhD: Université Paris-Saclay, CNRS, Institut Galien Paris-Saclay, Orsay, France; ³Fan Gao, PhD, David Paterson, PhD, Julien Reboud, PhD: Division of Biomedical Engineering, James Watt School of Engineering, University of Glasgow, Glasgow, United Kingdom; ⁴Luxin Yang, MSc, Lilian Nwosu, PhD, Aziza Elmesmari, MD, PhD, Iain B. McInnes, MBChB, PhD, Mariola Kurowska-Stolarska, PhD: School of Infection and Immunity, University of Glasgow, Glasgow, United

Kingdom; ⁵Gaetane Nocturne MD, PhD, Xavier Mariette MD, PhD: Rheumatology Department, Hôpital Bicêtre, Assistance Publique – Hôpitaux de Paris, Le Kremlin Bicêtre, France.

Additional supplementary information cited in this article can be found online in the Supporting Information section <http://onlinelibrary.wiley.com/doi/10.1002/art.42665>.

Author disclosures and graphical abstract are available at <https://onlinelibrary.wiley.com/doi/10.1002/art.42665>.

Address correspondence via email to Audrey Paoletti, PhD, at audrey.paoletti@inserm.fr; to Xavier Mariette, MD, at xavier.mariette@aphp.fr; or to Elias Fattal, PharmD, PhD, at elias.fattal@universite-paris-saclay.fr.

Submitted for publication May 16, 2023; accepted in revised form July 11, 2023.

has been shown in RA synovial macrophages and fibroblasts as well as in peripheral blood and synovial fluid CD14⁺ monocytes.^{9,10} We have previously demonstrated that the overexpression of miR-155 in RA blood monocytes led to a defect of monocyte polarization in anti-inflammatory macrophages.^{10,11}

What Is Already Known About This Topic

- Increased expression of miR-155 in monocytes of patients with rheumatoid arthritis could be responsible for the defect of monocyte polarization to anti-inflammatory macrophages.

What This Study Adds

- Treatment with an antagomiR-155-5p entrapped in polyethylene glycol liposomes in two mice models of mice with arthritis led to the restoration of the defect of blood monocytes polarization toward an anti-inflammatory macrophage in synovial tissue, reduction of immune cell infiltration in synovial tissue and improvement of arthritis, without any side effect on other immune cells.

How This Study Might Affect Research, Practice, or Policy

- This study is a proof of concept demonstrating that it is possible, thanks to liposome encapsulation, to address an antagomiR in monocytes and macrophages in joints at the site of inflammation, which can avoid systemic side effects. This strategy is promising in human disease.

Collagen-induced arthritis (CIA) is the most used murine model, in which breaking tolerance induces an immune-mediated inflammatory attack of the joints. It is an acute model that fulfills a few of the RA classification criteria, such as chronic inflammation and erosive arthritis. It is also highly variable depending on the quality of the type II collagen (CII) used and environmental factors and works efficiently only on the strain DBA/1OlaHsd. In contrast, K/BxN serum transfer arthritis (STA) in naïve C57BL/6 mice tends to be a fast-onset inflammatory model that mimics only the effector phase of RA. The STA model is a robust and reproducible model in many mice strains, with manifestations of arthritis occurring a few days after serum injection. The inflammatory response is driven by autoantibodies against the ubiquitously expressed self-antigen glucose-6-phosphate isomerase, leading to the formation of immune complexes that drive activation of different innate immune cells. Interestingly, both mouse models exhibit pro-inflammatory macrophage infiltration in the synovium that plays a key role in pathophysiology.^{6–8,12–15}

AntagomiRs can be used for neutralizing actions of miRs. However, they are relatively unstable in vivo, and chemical modifications may alter their biological properties. Furthermore, similar to conventional anti-inflammatory drugs, antagomiR-155-5p may cause severe nonmyeloid cell side effects, such as reduced protective immunity, fibrosis, or liver steatosis.¹⁶ Recently, partners of our group described in the CIA model an efficient strategy in which dexamethasone palmitate formulated as PEGylated (polyethylene glycol [PEG]) nanoparticles can extravasate through leaky endothelium in inflamed joints and be phagocytosed by monocytes and

macrophages.¹⁷ This occurred after a significant accumulation of labeled PEGylated nanoparticles, compared with low-score joints.¹⁷ Moreover, lipid nanoparticles, such as liposomes, can protect all types of nucleic acids against degradation.¹⁸ Based on robust evidence of the pathogenic role of miR-155 in human RA,¹¹ we have explored if an excess of miR-155-5p could drive inflammation in CIA and STA models and, consequently, evaluated the therapeutic utility of an antagomiR-155-5p encapsulated in PEGylated liposomes in these two mouse models.

MATERIALS AND METHODS

Mice. C57BL/6J mice were purchased from The Jackson Laboratory and subsequently bred in-house. DBA/1OlaHsd mice were purchased from Envigo. All mice were housed and maintained in a specific pathogen-free facility at the University of Glasgow for C57BL/6J mice and at the Faculty of Pharmacy Châtenay-Malabry for DBA/1OlaHsd mice under a 12-hour light/dark cycle in a temperature-controlled room with free access to water and food. In vivo experiments were performed under the protocol APAFIS#2842-2015110914248481v5.

For the CIA model, 10-week-old male DBA/1OlaHsd mice were injected intradermally at the base of the tail with an emulsion of grade chick CII and complete Freud's adjuvant. At day 21, the mice received a boost injection of the same composition. We determined the arthritic score and paw volume every two days after day 21 and euthanized mice at day 37. For the STA model, 8-week-old male C57BL/6J mice were injected at days 0 and 2 intraperitoneally with 150 μ L of arthritogenic serum (K/BxN mice) to induce arthritis. We determined the arthritic score and paw size every two days after day 0 and euthanized mice at day 5 during the strong inflammation phase. Clinical arthritis scores in CIA and STA mice were evaluated based on a visual scoring scale of the paws with evaluation of the erythema, swelling, and ankylosis of each paw with the following criteria: 0 = normal; 1 = swelling and/or redness of the paw or one digit; 2 = two digits swelling and/or redness; 3 = three digits swelling and/or redness; and 4 = severe arthritis of the entire paw and digit with skin shedding and wrist/ankle swelling. The total score was based on all four paws, with a maximum score of 16 for each mouse.

PEG liposomes production and characterization.

PEG liposomes were prepared using a thin-lipid film hydration method. The first step consisted of mixing together chloroform solutions of 1,2-dipalmitoyl-sn-glycero-3-phosphocholine, cholesterol, and 1,2-distearoyl-sn-glycero-3-phosphoethanolamine with conjugated PEG 2000 in a 62:35:3 M ratio and 1% of 1,1'-dioctadecyl -3,3,3',3'-tetramethylindotricarbocyanine perchlorate (DID) for fluorescently tagged liposomes. The chloroform present in the mixture was evaporated by rotary evaporator to form a dry lipid film. The resulting lipid film was hydrated with 10 mL of

RNase/DNase-free water. The solution was vortex mixed for 10 minutes followed by 15 minutes of sonication in ice.

Those empty PEG liposomes were then concentrated using Millipore columns Amicon (Merck) with 100 kDa cutoff to obtain 500 μ L after several centrifugations at 15°C for 20 minutes at 4,000 rpm before characterization. PEG liposomes were characterized by their size, polydispersity index, and zeta potential and were measured by dynamic light scattering using Nano ZS from Malvern (173° scattering angle) at 25°C. Samples were diluted 1:20 in water for the size and polydispersity index or in 1 mM NaCl solution for the zeta potential determination. Measurements were performed in triplicate. Phospholipid concentration within PEG liposome suspensions were also measured by enzymatic colorimetric method (Sigma-Aldrich-Merck) and PEG liposome suspensions were diluted to obtain a final concentration of 2.5 mg for antagomiR encapsulation. Briefly, antagomiR/protamine polyplexes were formed by mixing 2 nmol of antagomiR-control, control cyanine 3 (cy³), or 155-5p (MirVANA inhibitor second generation, Life Technologies #4464088) with 10 nmol of protamine (Merck). The antagomiR/protamine polyplexes were then mixed with 2.5 mg of PEG liposomes and five cycles of one minute in liquid nitrogen followed by two minutes in a water bath at 60°C were performed. To remove unencapsulated antagomiR, liposome suspensions were incubated with 10 μ L of ethylenediaminetetraacetic acid trypsin (Thermo Fisher Scientific) at 37°C for 10 minutes to break down any nonencapsulated antagomiR/protamine polyplexes. Free antagomiR and protamine were then removed by three successive centrifugal ultrafiltration phosphate buffered saline washes using 100 kDa cutoff Amicon columns (Merck). For encapsulation efficiency, we determined the unencapsulated antagomiR by Quantifluor (Promega) using antagomiR as standards. We obtained a range of 70.2% to 81.3% of encapsulated polyplexes.

Cell culture and PEG liposome uptake. Murine macrophage cell line RAW 264.7 obtained from ATCC was cultured in Dulbecco's modified Eagle Medium supplemented with 10% fetal bovine serum (FBS) and 100 IU/mL penicillin–streptomycin. Cultures were maintained at 37°C in a humidified atmosphere containing 5% CO₂. The uptake of PEG liposomes containing antagomiR-control or antagomiR-155-5p in RAW 264.7 cells was measured by quantitative reverse transcription polymerase chain reaction (RT-qPCR). Cells were seeded in 12-well plates at 8×10^4 cells/well and incubated for 24 hours to reach 80% confluency. PEG liposomes were added at $1 \times (1.5 \text{ nmol}/100 \mu\text{L})$ to $2.5 \times$ and $5 \times$, and plates were incubated for 48 hours. The medium was then removed, and cells were washed with PBS-1X and frozen at –80°C until RNA extraction and RT-qPCR analysis.

Epifluorescence imaging for biodistribution in CIA mice. Tagged DID 1% liposomes as described above were diluted at 2.5 in PBS-1X to optimize fluorescence in mice. For imaging, mice were anesthetized in an induction chamber with

3% isoflurane and maintained with 2% isoflurane. DBA/10IaHsd control and arthritis-induced mice were injected with 100 μ L by retro-orbital injection at day 27 and imaged at 1, 2, 4, 24, and 48 hours after injection on the dorsal and ventral positions. At day 29, the animals were euthanized, and the liver, spleen, kidney, heart, lung, and intestines were collected. The epifluorescence of the different organs was then analyzed using an IVIS Lumina III machine (Caliper Life Science) equipped with a heated stage. The setting for imaging was automatic phototime exposition, medium binning, an excitation wavelength of 640 nm, and an emission wavelength of 710 nm. Living Image Software (version 4.5.5, Caliper Life Science) was used to visualize the fluorescence images and quantify intensity using regions of interest and subtraction of the background fluorescence. Background fluorescence was determined on the oral mucosa, skin of the feet, and prepuce.

Therapeutic treatment of antagomiR-155-5p in CIA

and STA mice. For systemic injection, DBA/10IaHsd-CIA mice were injected on days 22, 29, 36, and 41, with 43.4 nmol per injection of antagomiR-155-5p, antagomiR-control, or PBS. DBA/10IaHsd-CIA and C57BL/6J-STA mice were injected on days 30, 32, and 34 (CIA) or on days 1, 2, 3, and 4 (STA) and received intravenously 1.5 nmol per injection of antagomiR-155-5p or antagomiR-control encapsulated in PEG liposomes. Mice were evaluated every 2 days based on a visual scoring scale of the paws with evaluation of the erythema, swelling, and ankylosis of each paw (score 1–4).

Cells isolation, monocytes differentiation in macrophages and synovium tissues experimental protocol.

Single-cell suspensions were prepared by standard mechanical disruption for liver and spleen and filtered through, respectively, 70 or 40 μ m nylon cell strainers. Splenocytes were counted, and monocytes, B cells, and T cells were isolated using CD11b microbeads, a B cells isolation kit, and a Pan T cells isolation kit according to the manufacturer's instructions (Miltenyi Biotec) to achieve a purity of >75%. Crushed liver or isolated splenocytes were stored at –80°C until analysis.

To generate bone marrow-derived macrophages (BMDMs), bone marrow cells from the femurs and tibias of mice were collected and isolated by centrifugation. Briefly, femurs and tibias were folded in 0.2 mL Eppendorf holed by a 23 G needle and centrifuged at 4°C in 3,000 g for 1 minute in a 1.5 mL Eppendorf containing 200 μ L of PBS-1X. Cells were filtrated on a 70 μ m nylon cell strainer, and red blood cells were lysed in a red blood cell buffer (Biolegends). Cells were washed, and bone marrow monocytes were isolated using a monocytes isolation kit for bone marrow according to the manufacturer's instruction (Miltenyi Biotec) to achieve a purity of >80%. Then monocytes were washed, counted, and stored at –80°C. For experimental works, 250,000 cells/mL were seeded in six-well plates and cultured in

Dulbecco's modified Eagle Medium supplemented with 100 IU/mL penicillin–streptomycin, 10% FBS, and macrophage colony-stimulating factor (M-CSF; 10 ng/mL) for five days. Interleukin (IL)-4 (20 ng/mL) was then added for 24-hour treatment. Cells were washed for analysis, and supernatant were collected and stored at -80°C until analysis.

Mouse synovia were collected and transferred in Eppendorf coating with 0.4% bovine serum albumin, with 1 mL of RPMI 1640 media supplemented with 100 IU/mL penicillin–streptomycin and 10% L-glutamine, 15 μL liberase (5 mg/mL; Roche) and 100 μL DNaseI (10 $\mu\text{g}/\text{mL}$; Roche). After 45 minutes incubation under 150 rpm shaking at 37°C , cells were filtered through a 100 μm nylon cell strainer, washed, and stained.

Flow cytometry and enzyme-linked immunosorbent assay. For bone marrow monocyte purity, cells were saturated with Fc block and incubated for 30 minutes at 4°C with anti-CD11b and anti-Ly6C antibodies. After monocyte polarization in macrophages by M-CSF+IL-4 for alternative activated macrophage (M2) phenotype, cells were collected in 100% FBS and scratched, washed once with PBS-1X, saturated with Fc block, and incubated for 30 minutes at 4°C with anti-F4/80, anti-CD11b, and anti-CD206 (gating strategy in Supplementary Figures 1 and 2C). For monocyte, B cell, and T cell spleen purity, cells were saturated with Fc block and incubated for 30 minutes at 4°C with anti-B220 for B cells; anti-CD3, anti-CD4, and anti-CD8 for T cells; and anti-CD11b and anti-Ly6C antibodies for monocytes (gating strategy in Supplementary Figure 2D, 2E and F). For mice synovial tissue staining, cells were saturated with Fc block and incubated for 30 minutes at 4°C with anti-CD45, DUMP channel anti-CD3-CD19-NK.1.1-Ly6G, anti-CD11b, anti-F4/80, anti-CD64, anti-Ly6C, anti-major histocompatibility complex class II, anti-MerTK, anti-CD163, anti-CD206, and anti-CX3C motif chemokine receptor 1 (CX3CR1) (gating strategy in Supplementary Figure 2B).

For blood analysis staining, 50 μL of blood were collected in PBS-1X solution containing 1 nM ethylenediaminetetraacetic acid. Cells were pretreated with red blood cell lysis at $1\times$ for 5 minutes at room temperature, followed by saturation with Fc block, and incubated for 30 minutes at 4°C with anti-CD45, DUMP channel anti-CD3-CD19-NK.1.1-Ly6G-CD11c, anti-CD11b, and anti-Ly6C. The indicated antibodies and isotype-matched antibodies used were obtained from Biolegend. Stained cells were acquired by using BD FACSCantoI, BD LSRII, or SORP BD Fortessa flow cytometer (BD Biosciences) and analyzed with Flowjo V10. Doublets were excluded by the appropriate forward/side scatter gates, whereas dead cells were excluded using Fixable viability dye eFluor 780 (ref 65-0865-18 life technologies) for BMDM and cell purity or Live-Dead BUV496 (ref L23105 life technologies) for blood and synovial staining. IgG–IgM and IgA concentration in plasma samples and IL-10 concentration in cell-free supernatants after a six-day culture of BMDM were measured

according to the manufacturer's instructions (Thermo Fisher Scientific).

qPCR and statistical analysis. Total RNA from RAW 264.7 liver and spleen monocytes, B cells, T cells, bone marrow monocytes, and monocyte polarization in M1 or M2 phenotype macrophages was extracted with the GeneJET kit (Thermo Fisher Scientific) according to manufacturer specifications for miR-155-5p, suppressor of cytokine signaling 1 (SOCS-1), CCAAT enhancer binding protein β (CEBP- β), macrophage receptor with collagenous structure (MARCO), YM-1, PU.1, SH2 domain-containing inositol phosphatase 1 (SHIP-1), PR domain zinc finger protein 1 (PRDM1), interferon γ (IFN- γ), and IL-4 detection. The quantification of messenger RNA (mRNA) expression was determined by TaqMan real-time PCR and miRNA by the miScript II SYBR Green PCR kit according to the manufacturer's instructions. The amounts of SOCS-1, CEBP- β , MARCO, YM-1, PU.1, SHIP-1, PRDM1, IFN- γ , and IL-4 were normalized to the endogenous glyceraldehyde 3-phosphate dehydrogenase, and miR-155-5p expression was normalized to miR-25 and RNU6.¹⁹ The efficiency of PCR using TaqMan probes was performed using a serial dilution of amplicons and verification of the melting curve for SYBR Green. Calculations of mRNA and miRNA expression levels were performed using the comparative cycle threshold method ($\Delta\Delta\text{Ct}$). The data were analyzed by using Graph Pad Prism version 9.3.1. Data were tested by unpaired *t*-test for two groups and the Kruskal-Wallis test with multiple comparisons for multiple groups, expressed as mean \pm SEM with individual plot values.

RESULTS

Impaired maturation of bone marrow monocyte polarization in anti-inflammatory macrophages in mice with arthritis. To explore whether the defect of monocyte polarization in anti-inflammatory macrophages is present in CIA mice, 10-week-old male DBA/10Jahsd mice were injected with an emulsion of grade chick CII and complete Freund's adjuvant to induce arthritis, and we analyzed bone marrow monocyte polarization at day 36. For the STA model, eight-week-old male C57BL/6J mice were injected intraperitoneally at days 0 and 2 with 150 μL of arthritogenic serum, and we analyzed monocyte polarization at day 5 (Figure 1A). After culture in medium supplemented with M-CSF for five days and 24 hours of IL-4 stimulation for M2 polarization (gating strategy in Supplementary Figure 1A and B), we did not find any change in the expression of pan-macrophage markers CD11b-F4/80 in CIA and STA mice (Figure 1B). After validation of M2 and M1 markers of macrophages in these two mouse models, we demonstrated a defect of M2 polarization in mice with arthritis with a lower CD206 expression (Figure 1C), a decrease of IL-10 production (Figure 1D), and a decrease of YM-1 relative expression

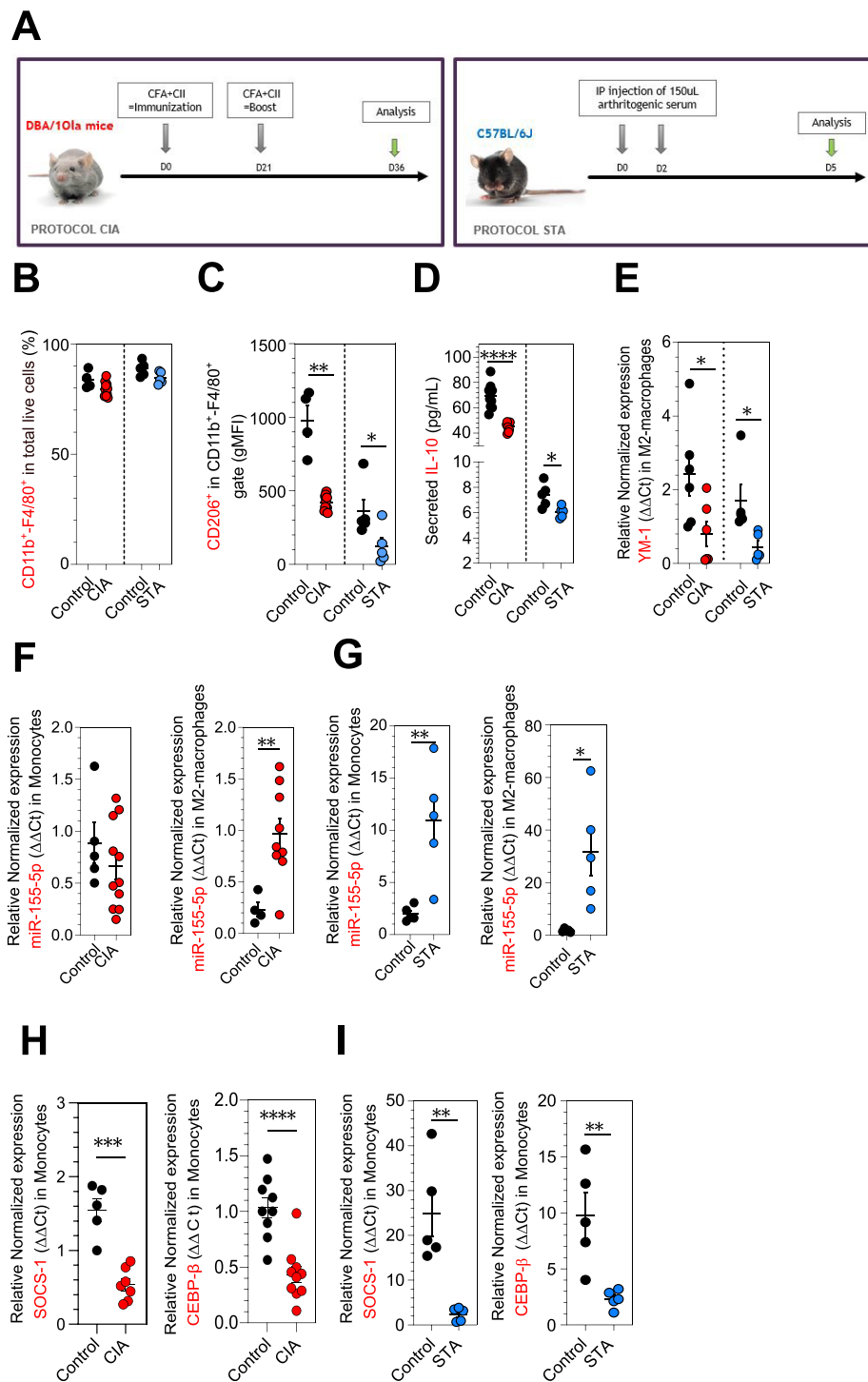


Figure 1. Ex vitro monocytes polarization in CIA and STA mice and miR-155-5p implication in monocytes polarization in M2. **(A)** Experimental timeline of immunization procedure and development of arthritis in two preclinical models. **(B)** The differentiation of sorted bone marrow monocytes to bone marrow-derived macrophage M2 was assessed in CIA ($n = 11$ red dots) and STA ($n = 5$ blue dots) arthritic models, with their respective control mice ($n = 11$ for CIA and $n = 5$ for STA black dots), by flow cytometry with anti-CD11b and anti-F4/80 antibodies. Specific markers of M2 macrophage polarization were assessed: **(C)** CD206, **(D)** IL-10 secretion in cell culture supernatant, and **(E)** YM-1 relative expression. miR-155-5p expression on bone marrow monocytes and bone marrow-derived macrophage M2 was determined by quantitative real-time polymerase chain reaction on **(F)** CIA and **(G)** STA mice models. Target mRNA SOCS-1 and CEBP- β relative expressions are shown on **(H)** CIA monocytes and **(I)** STA monocytes. The data are shown as symbols and mean \pm SEM and were compared by unpaired t -test. * $P < 0.05$; ** $P < 0.01$; *** $P < 0.001$; **** $P < 0.0001$. CEBP- β , CCAAT enhancer binding protein β ; CFA, Freund's complete adjuvant; CIA, collagen-induced arthritis; CII, type II collagen; gMFI, geometric mean fluorescence intensity; IL-10, interleukin 10; IP, intraperitoneal; M2, alternative activated macrophage; miR, microRNA; SOCS-1, suppressor of cytokine signaling 1; STA, serum transfer arthritis.

(Figure 1E) compared with controls. Thus, the CIA and STA models impaired maturation of bone marrow monocytes in anti-inflammatory macrophages similar to that observed in patients with RA.

miR-155-5p is overexpressed in monocytes and M2 macrophages in mice with arthritis. To follow up our previous publication on the link between miR-155 overexpression in monocytes and macrophages and the defect of monocyte polarization in anti-inflammatory macrophages in human RA,¹¹ we analyzed mature miR-155-5p expression and demonstrated up-regulation in CIA M2 macrophages (Figure 1F), STA monocytes, and M2 macrophages (Figure 1G) compared with controls. Moreover, we also found down-regulation of two major mRNA targets of miR-155-5p and a regulator of monocyte polarization in anti-inflammatory macrophages SOCS-1 and CEBP β in arthritic mice (Figure 1H–I). These results confirmed the translational potential of findings observed in human RA toward arthritis murine models and suggested the utility of these mouse models for testing specific therapeutic approaches, such as antagomiR-155-5p encapsulated in PEG liposomes for correcting such abnormalities.

PEG liposome accumulates on joints of arthritic mice. We chose liposomes as potent vectors to deliver fragile hydrophobic molecules such as antagomiRs. Once injected into the blood circulation, liposomes passively extravasate and accumulate at the sites of inflammation.²⁰ This improved drug distribution typically leads to an increase in drug efficacy and a reduction of side effects and toxicity.^{21–23} We produced PEG liposomes labeled with 1% of lipophilic tracer DID with fluorescence excitation and emission spectra that allow optical imaging in the near infrared window. CIA or control DBA/10LaHsd mice were injected at day 27 with empty DID1% PEG liposomes. Dorsal and ventral position imaging was performed at 1, 2, 4, 24, and 48 hours after liposome injection using an *in vivo* imaging system (Figure 2A and B). Images obtained demonstrated that DID1% PEG liposomes can infiltrate the inflamed paw joints and accumulate in highly inflamed paws (scores 2–4) compared with mildly inflamed paws (score 1) and healthy paws (score 0; Figure 2B and C). Moreover, DID1% PEG liposomes were still detected in paw joint and in some organs, such as the liver and spleen, 48 hours after the injection (Figure 2D and E), suggesting prolonged action.

PEG liposomes encapsulating antagomiR-155-5p ameliorate arthritis. In the CIA mice model, a preliminary experiment consisting of the systemic delivery of 43.4 nmol per injection of free antagomiR-155-5p at days 22, 29, 36, and 41 did not change the arthritic score (Supplementary Figure 3A). Because PEG liposomes were nicely distributed in inflamed joints, we proceeded with its encapsulation in this formulation. We first determined the efficiency of antagomiR encapsulated in PEG

liposomes *in vitro* in cells. We incubated murine macrophages (RAW 264.7) with PEG liposomes encapsulating antagomiR-control or antagomiR-155-5p for 24 hours at 37°C, with the rate 70.2% to 81.3% of polyplex-antagomiR entrapped in liposomes. We determined the relative normalized expression of SOCS-1 and CEBP- β by RT-qPCR. We demonstrated the same efficiency to decrease relative expression of SOCS-1 and CEBP- β with 1 \times (1.5 nmol/100 μ L), 2.5 \times , and 5 \times (Supplementary Figure 3B). We showed, in a CIA model with high inflammation, that therapeutic injection at days 30, 32, and 34 of antagomiR-155-5p encapsulated in PEG liposomes (1.5 nmol/100 μ L) reduced the arthritis score and paw volume significantly only at day 36 but not at other time points (Figure 3A–C). The absence of difference at other time points might be because the arthritis score was very high and the concentration of 1.5 nmol of antagomiR-155-5p in PEG liposome could be limited in case of high inflammation. We confirmed in the STA mice model that early injection of PEG liposomes containing antagomiR-155-5p (1.5 nmol/100 μ L) led to a significant reduction of the arthritis score and paw size (Figure 3D–F).

Restoration of monocyte defect in differentiation into anti-inflammatory macrophages after treatment *in vivo* with PEG liposomes encapsulating antagomiR-155-5p. We next investigated whether the decrease of the arthritis score and paw volume/size in CIA and STA mice could be associated with the restoration of the monocyte polarization into anti-inflammatory macrophages. For this purpose, we isolated monocytes from the bone marrow of mice with arthritis treated with PEG liposomes encapsulating antagomiR-control or antagomiR-155-5p. We found no significant change in the pan-macrophage marker CD11b-F4-80 expression (Figure 4A and Supplementary Figure 3D). We observed a restoration of monocyte polarization into M2 macrophage with an increase of CD206, IL-10 secretion, and YM-1 expression (anti-inflammatory markers) (Figure 4B and Supplementary Figure 3E) and a decrease of MARCO (pro-inflammatory marker) (Figure 4C and Supplementary Figure 3F). This suggests efficient delivery of antagomiR-155-5p by PEG liposomes to monocytes and macrophages (Supplementary Figure 3C and G).

***In vivo* treatment with PEG liposomes encapsulating antagomiR-155-5p impacts synovial homeostasis.** To determine if the inhibition of miR-155-5p had an impact on resident macrophages and migratory monocytes in synovial tissue, we extracted on day 5 the synovial tissue of STA mice (gating strategy in figure Supplementary Figure 2A and B). We demonstrated that treatment with antagomiR-155-5p loaded in PEG liposomes induced a decrease in CD45⁺ immune cell infiltration (Figure 4D) and of the pool of B, T, natural killer, and neutrophils cells (Figure 4F). Interestingly, we did not find any change in the synovial infiltration of the CD45[−] cells, probably reflecting epithelium–fibroblast cells (Figure 4E).

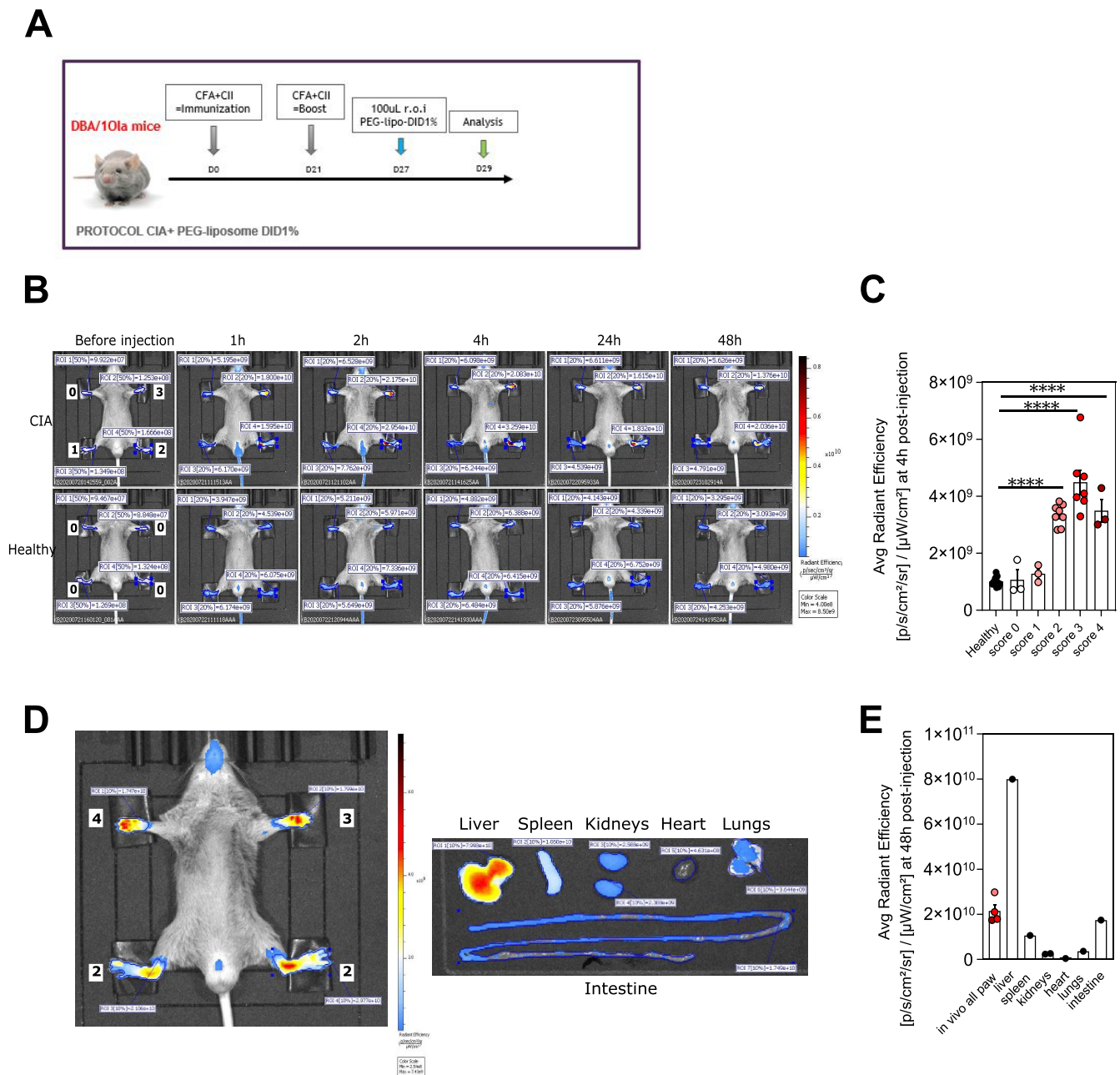


Figure 2. Accumulation in vivo of DID 1%-PEG-liposomes in inflamed joints. **(A)** Experimental timeline of immunization and DID-PEG-liposomes. Ten-week-old male DBA/10laHsd mice were injected intradermally at the base of the tail with an emulsion of grade chick type II collagen and complete Freud's adjuvant. At day 21, mice received a boost injection of the same composition. After intravenous injection at day 27 of fluorescent PEG liposomes the evolution of the near infrared signal (dorsal view) in healthy mice ($n = 3$) and CIA mice ($n = 6$) was monitored according to the arthritis score for each paw. In vivo representative images of one mouse per group before and after injection with DID 1%-PEG-liposomes at 1, 2, 4, 24, and 48 hours. **(B)** The score of each paw is indicated in white squares on the "before injection" image. **(C)** The average radiant efficiency four hours after intravenous injection with DID 1%-PEG-liposomes in paws segregated based on their arthritis score. In vivo representative images of one CIA mouse after 48 hours injection with DID 1%-PEG-liposomes. The score of each paw is indicated in white squares on the "before injection" image. **(D)** Ex vivo organ representative images of the same CIA mice with the same sequence and scale and average radiant efficiency on CIA mice ($n = 6$) demonstrated **(E)** the comparison between paw, liver, spleen, kidneys, heart, lung, and intestine biodistribution of DID 1%-PEG-liposomes. Data are shown as symbols and mean \pm SEM and were compared by ordinary one-way analysis of variance with multiple comparisons. **** $P < 0.0001$. CFA, Freud's complete adjuvant; CIA, collagen-induced arthritis; CII, type II collagen; DID, 1,1'-dioctadecyl-3,3',3',3'-tetramethylindotricarbocyanine perchlorate; PEG, polyethylene glycol; ROI, region of interest.

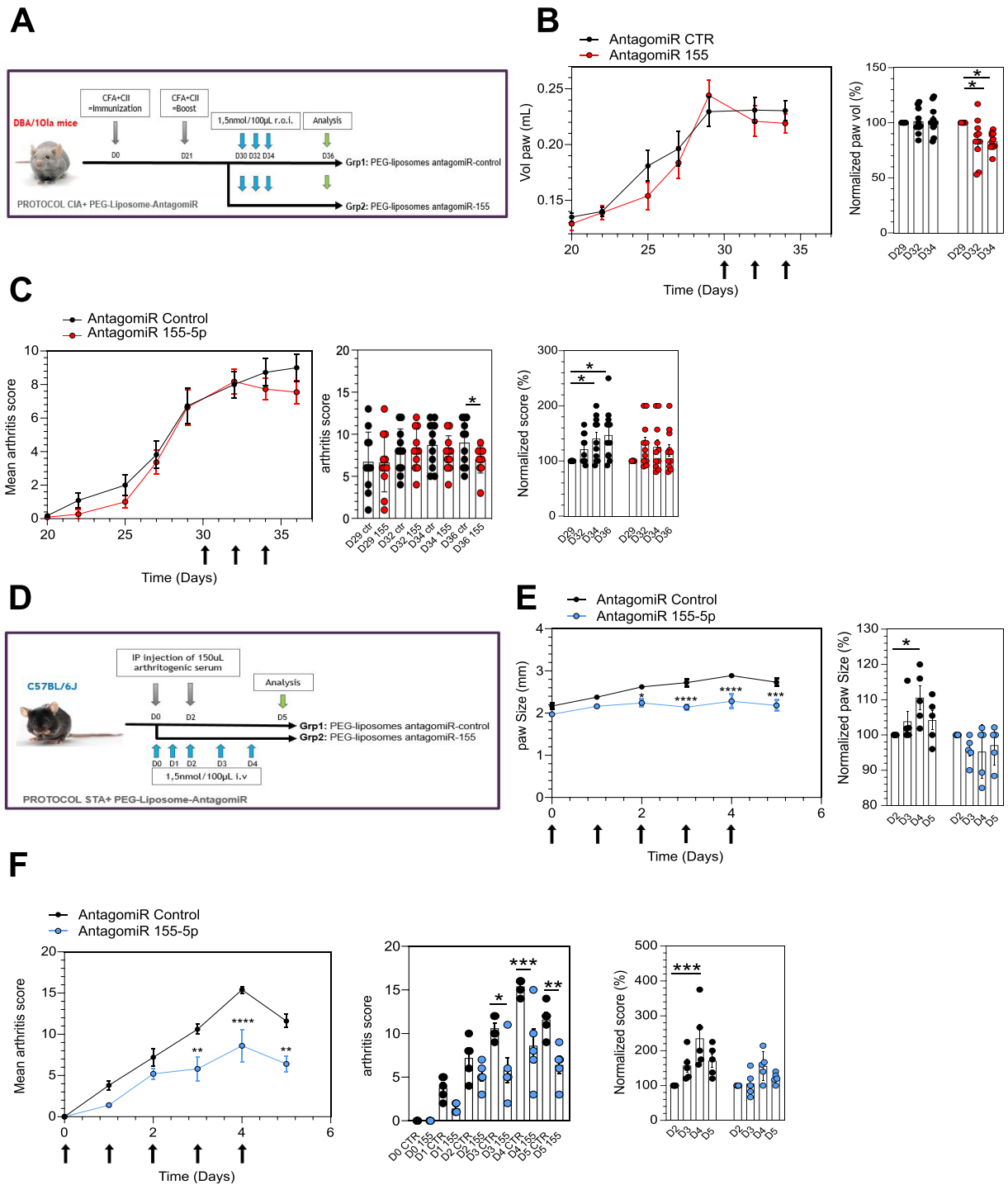


Figure 3. Treatment of CIA and STA mice with PEG liposomes containing antagomiR-control or antagomiR-155-5p. Experimental timeline of immunization and PEG liposomes injection in (A) CIA model or (D) STA. For CIA mice (red dots), antagomiR-control or 155 entrapped in PEG liposomes are intravenously injected on days 0, 1, 2, 3, and 4. Hind paw volume was measured with a plethysmometer for (B) CIA model or caliper for (E) STA. (C and F) Mice were evaluated every two days, based on a visual scoring scale of the paws with evaluation of the erythema, swelling, and ankylosis of each paw (score 1–4). Data are shown as symbols and mean and error \pm SEM and were compared by ordinary two-way analysis of variance with multiple comparisons or by one-way ordinary analysis of variance with multiple comparisons. We use a classical normalization formula where the data mean of D29 for CIA and D2 for STA mice of each group of injection is equal to 100%. * $P < 0.05$; ** $P < 0.01$; *** $P < 0.001$; **** $P < 0.0001$. CFA, Freund’s complete adjuvant; CIA, collagen-induced arthritis; CII, type II collagen; CTR, control; IP, intraperitoneal; IV, intravenous; miR, microRNA; PEG, polyethylene glycol; ROI, region of interest; STA, serum transfer arthritis.

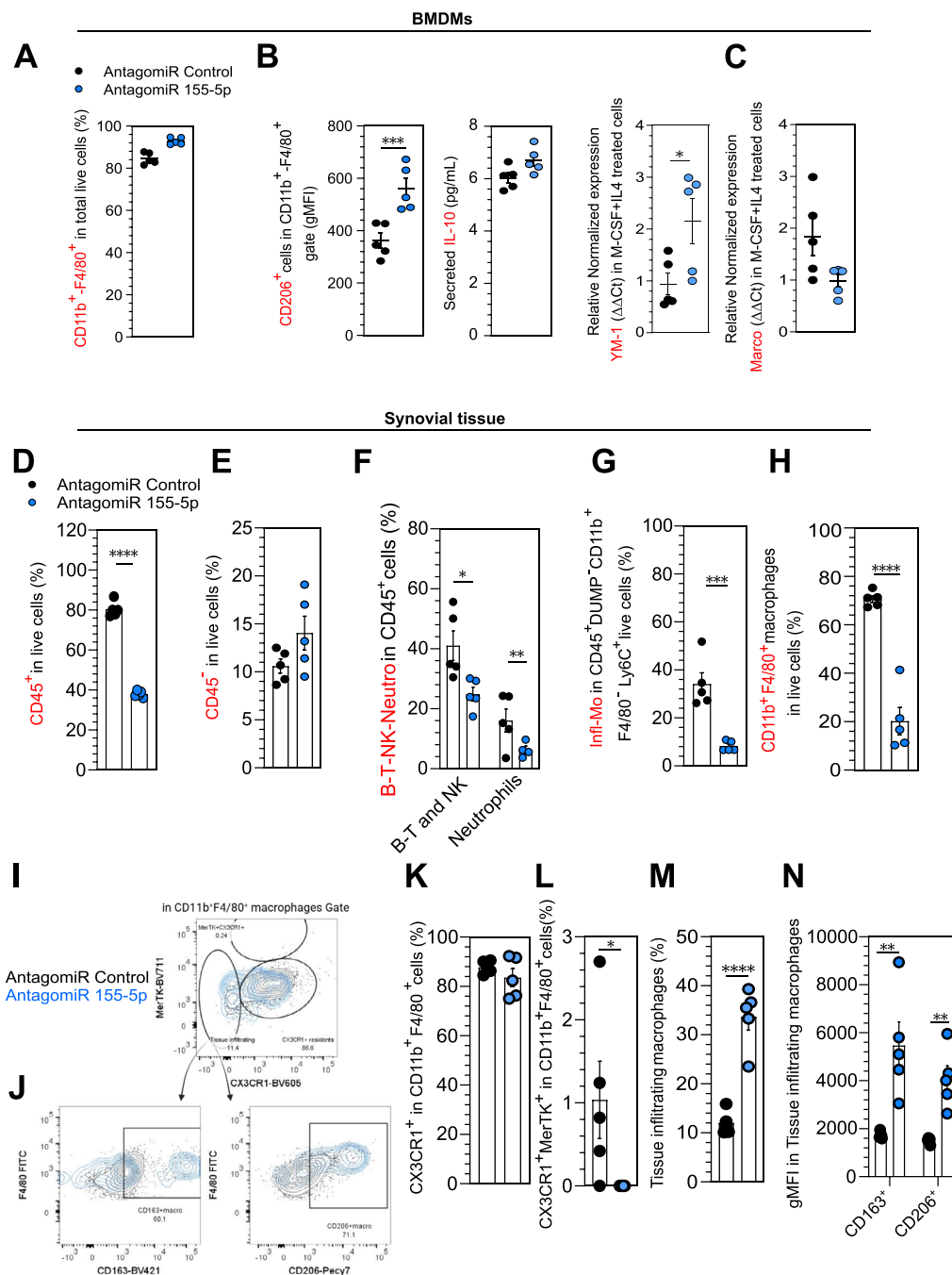


Figure 4. Ex vitro monocyte polarization in STA mice and ex vivo synovial homeostasis after treatment with PEG liposomes containing an antagomiR-155-5p. (A–C) The differentiation of sorted bone marrow monocytes to BMDM-M2 was assessed in STA (blue dots) arthritic model with respective control mice (black dots) by flow cytometry with anti-CD11b and anti-F4/80 antibodies. (B) Specific markers of M2 macrophage polarization were assessed: CD206, IL-10 secretion in cell culture supernatant, and YM-1 relative expression. (C) Relative expression of M1 macrophages marker MARCO was determined by Taqman probes. (D–N) Synovial tissue cells were assessed by flow cytometry analysis using anti-CD45, DUMP channel: CD19-CD3-NK1.1-LY6G, anti-CD11b, anti-F4/80, anti-major histocompatibility complex class II, anti-CD64, anti-LY6C, anti-MerTK, anti-CD163, anti-CD206, and anti-CX3CR1. (D) Determination of CD45⁺ cells, (E) CD45⁻, (F) DUMP channel⁺ cells (B-T-NK and Neutro), (G) inflammatory monocytes, and (H) macrophage infiltration in synovial tissue. (I and K) Exploration of residents CX3CR1⁺, (I and L) protective lining MerTK⁺, (J and M) tissue-infiltrating CD206⁺ or CD163⁺ macrophages. (N) Tissue-infiltrating macrophages. Data are shown as symbols and mean \pm SEM and were compared by unpaired *t*-test. **P* < 0.05; ***P* < 0.01; ****P* < 0.001; *****P* < 0.0001. BMDM, bone marrow-derived macrophage; B-T-NK, B, T, and natural killer cells; CX3CR1, CX3C motif chemokine receptor 1; FITC, fluorescein isothiocyanate; gMFI, geometric mean fluorescence intensity; IL-10, interleukin 10; IL4, interleukin 4; M2, alternative activated macrophage; MARCO, macrophage receptor with collagenous structure; M-CSF, macrophage colony-stimulating factor; miR, microRNA; PEG, polyethylene glycol.

There are two main subsets of blood monocytes in mice: inflammatory monocytes, which express $CD11b^+Ly6C^{Hi}$, and patrolling monocytes that express $CD11b^+Ly6C^{Lo}$. We demonstrated a significant decrease in synovial tissue of $Ly6C^+$ inflammatory monocytes that comes from the blood after treatment with PEG liposomes (cluster $CD45^+DUMP^-Ly6C^+CD11b^+F4/80^-CD64^-$) (Figure 4G). Moreover, in mice treated with PEG liposomes encapsulating antagomiR-155-5p, a decrease in $CD11b^+F4/80^+$ macrophages population was observed (Figure 4H). In the $CD11b^+F4/80^+$ macrophage population, there was no change in the lining resident macrophages $CX3CR1^+$ and no restoration of the protective lining macrophages $CX3CR1^+MerTK^+$ after treatment (Figure 4I-K) compared with control mice (Supplementary Figure 2B). We observed an increase of the tissue-infiltrating macrophages $CD11b^+F4/80^+CX3CR1^-MerTK^-$ after treatment with liposomes

encapsulating antagomiR-155-5p (Figure 4L). In the tissue-infiltrating macrophage population, we found new populations of $CD11b^+F4/80^+CD206^{high}/CD11b^+F4/80^+CD163^{high}$ cells, probably deriving from blood monocytes (Figure 4J-M) and suggesting a restoration of the monocyte defect in M2 macrophage polarization after treatment with an antagomiR-155-5p encapsulated in PEG liposome.

Internalization of antagomiR-155-5p-tagged cy^3 on blood monocytes in mice with arthritis. We explored the impact of PEG liposomes encapsulating antagomiR labeled with cy^3 on blood monocytes at day 2 and on synovial macrophages at day 5 (Figure 5A). We detected the cy^3 signal only in blood monocytes $CD11b^+Ly6C^+$ and not in other cells (DUMP⁺ cells) or noninjected mice (Figure 5B and E). Moreover, we found more cy^3 signals in blood monocytes in STA mice than in control mice,

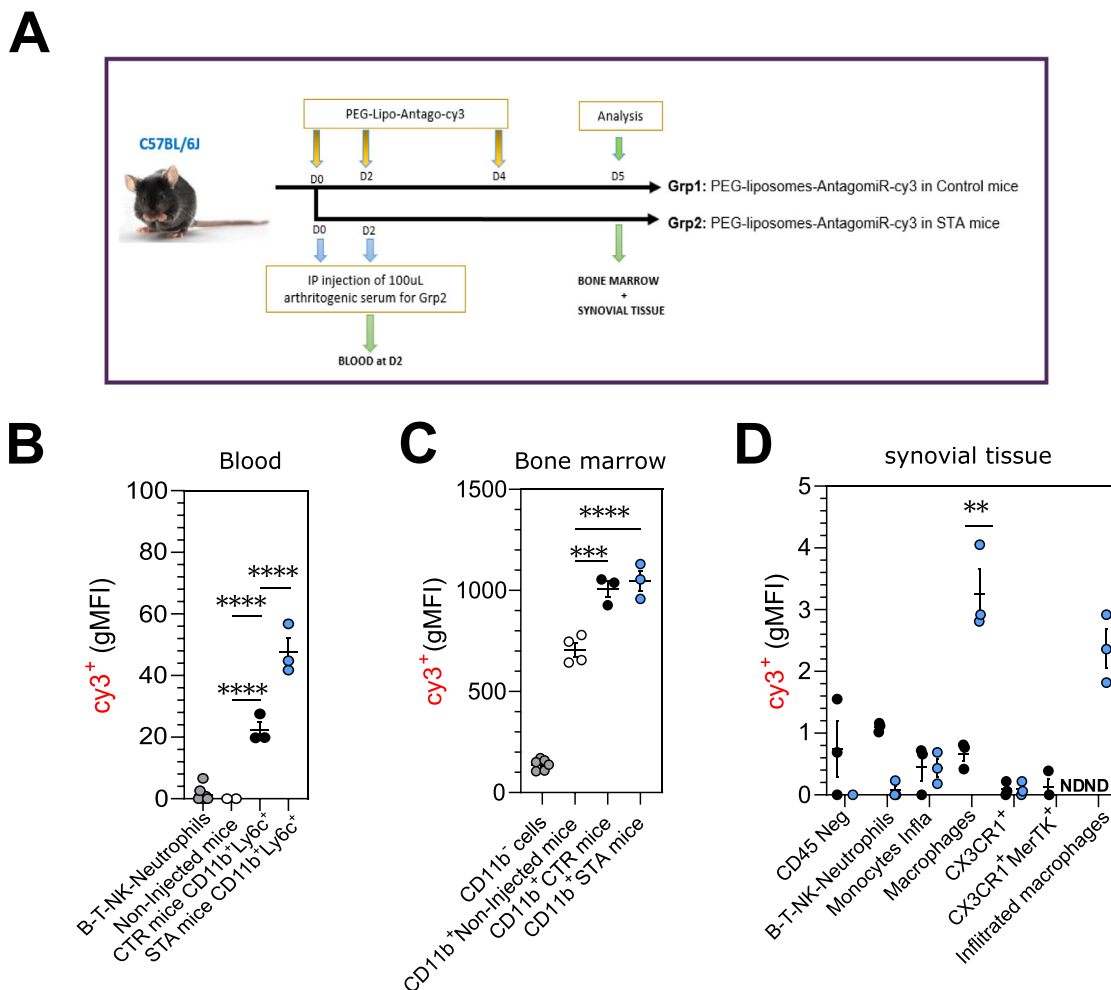


Figure 5. Specific biodistribution ex vivo of PEG liposomes in monocyte macrophage cells. (A) Experimental timeline of immunization and PEG liposomes containing antagomiR-control- cy^3 injection in STA model. Determination of cy^3 staining in (B) blood monocytes, (C) bone marrow $CD11b^+$ monocytes, or (D) synovial tissues cells and macrophages. Data are shown as symbols and mean \pm SEM and were compared by unpaired *t*-test. $**P < 0.01$; $***P < 0.001$; $****P < 0.0001$. B-T-NK, B, T, and natural killer cells; CTR, control; $CX3CR1$, $CX3C$ motif chemokine receptor 1; cy^3 , cyanine-3; gMFI, geometric mean fluorescence intensity; IP, intraperitoneal; miR, microRNA; ND, not determined; PEG, polyethylene glycol; STA, serum transfer arthritis.

probably because of the shift of Ly6C fluorescence intensity in STA mice. Thus, we suggest that PEG liposomes are more directed to the Ly6C^{high} monocyte population.

At day 5, we collected bone marrow and synovium tissues. In bone marrow, we detected the cy³ signal in the CD11b⁺ monocyte/macrophage population without any difference between control mice and STA (Figure 5C and F). In synovium, we demonstrated a slight cy³ signal in STA macrophages F4/80⁺CD11b⁺ and no cy³ signal in the resident macrophages CX3CR1⁺ and in the protective population CX3CR1⁺MerTK⁺. Because the tissue-infiltrating macrophages are present only in STA mice, we demonstrated the presence of a cy³ signal in these macrophages (Figure 5D and G). Altogether, these results suggest that PEG liposomes are first internalized by blood monocytes CD11b⁺Ly6C^{high} and hitchhike within these monocytes, which go into the synovium and are polarized in macrophages CD11b⁺F4/80⁺.^{24,25}

In vivo treatment with PEG liposomes encapsulating antagomiR-155-5p has a limited impact on other immune cells. The objective of the encapsulation of antagomiRs within PEG liposomes was to specifically direct them to monocytes and macrophages (linked to phagocytosis) and to spare other immune cells and, as much as possible, liver and spleen macrophages. As antagomiR-155-5p may cause severe nonmyeloid cell side effects on others immune cells, we analyzed the impact of antagomiR-155-5p or antagomiR-control effect on Kupffer cells, sorted CD11b⁺ monocytes, and B and T cells of the spleen (Supplementary Figure 2D–F). We were able to demonstrate that treatments with antagomiR-155-5p encapsulated in PEG liposomes had no impact on the percentage of these cells in CIA (Supplementary Figure 2C–F) or on their absolute number. Likewise, antagomiR-155-5p encapsulated in PEG liposomes had no impact on the main targets of miR-155 in sorted T cells, such as IFN- γ , IL-4, SOCS-1, and CEBP- β (Figure 6C and Supplementary Figure 5C). In sorted B cells, antagomiR-155-5p encapsulated in PEG liposomes did not impact the relative expression of PU.1, SHIP-1, PRDM1, SOCS-1, CEBP β (Figure 6D and Supplementary Figure 5D), and immunoglobulin secretion in mice plasma cells (Figure 6E and Supplementary Figure 5E), suggesting that antagomiR-155-5p encapsulated in PEG liposomes have no or minor effect on T and B cells.

We then studied the effect of antagomiR-155-5p encapsulated in PEG liposomes on liver and spleen monocytes and macrophages of CIA and STA mice. We found a paradoxical decrease in SOCS-1 and CEBP- β in the liver macrophages of CIA mice and a trend in STA mice (Figure 6A and Supplementary Figure 5A). Conversely, we found a trend for the increase of SOCS-1 and CEBP- β , which was the expected action of the antagomiR-155-5p in spleen monocytes (Figure 6B and Supplementary Figure 5B). Thus, encapsulated in PEG liposomes, antagomiR-155-5p displayed only a limited impact on spleen

monocytes and liver macrophages despite the high accumulation in the liver observed by optical imaging (Figure 2D and E).

DISCUSSION

Using reverse translational science, we confirmed our previous observations in human RA¹⁰ and found in two preclinical mouse models of RA a defective bone marrow monocyte polarization into anti-inflammatory macrophages (M2), with a decrease of CD206, YM-1 expression, and secretion of IL-10. As in humans, we found that this defect was associated with an increase of miR-155-5p in monocytes and anti-inflammatory macrophages in both mouse models. Because BMDMs and synovial macrophages have different transcriptional profiles,^{5,26} we also studied subsets of synovial macrophages and BMDMs. Subsequently, we demonstrated that treatment with an antagomiR-155-5p encapsulated in PEG liposomes was able to decrease joint inflammation, restore bone marrow monocyte polarization into anti-inflammatory macrophages, reduce immune cell infiltration in synovial tissue, increase the CD206⁺ and CD163⁺ tissue-infiltrating macrophages, and decrease expression of the mRNA's target of miR-155-5p.

miRs indeed represent a class of small endogenous noncoding RNA molecules that play an important role in posttranscriptional regulation of gene expression. The critical role of miR-155 in RA has been further demonstrated in mice, as subcutaneous injection of collagen in *miR-155*^{-/-} mice did not lead to the development of clinical signs of arthritis, such as increases in paw volume and swelling.²⁷ AntagomiR-155-5p are chemically modified nucleic acids designed to bind miR-155-5p (100% coverage of miRBase V21). Here, we demonstrated that antagomiR-155-5p encapsulated in PEG liposomes to treat CIA and STA mice lead to a reduction in arthritis score and a restoration of the defect of monocyte polarization in anti-inflammatory macrophages with increases of CD206, YM-1, and IL-10 secretion and a decrease of MARCO.

Moreover, PEG liposomes were specifically taken up by blood and bone marrow monocytes CD11b⁺Ly6C^{high}, which were increased in STA mice, and had no or minor effects on liver macrophages, spleen monocytes, B cells, T cells, and synovial resident macrophages. Similar to most of the preclinical experiments in mouse models of arthritis,²⁸ we found that the prophylactic injection of PEG liposomes containing antagomiR-155-5p was more efficient for decreasing inflammation and arthritic score than a curative strategy. However, in both arthritis models, prophylactic or curative treatment with a small concentration of antagomiR-155-5p (1.5 nmol/100 μ L) induced a restoration of monocyte defect in anti-inflammatory macrophages and had an impact on infiltrating macrophages, although the treatment did not impact on resident macrophages and on CD45-negative cells, probably reflecting epithelium-fibroblast cells. The relative expression of miR-155-5p in monocytes and macrophages is

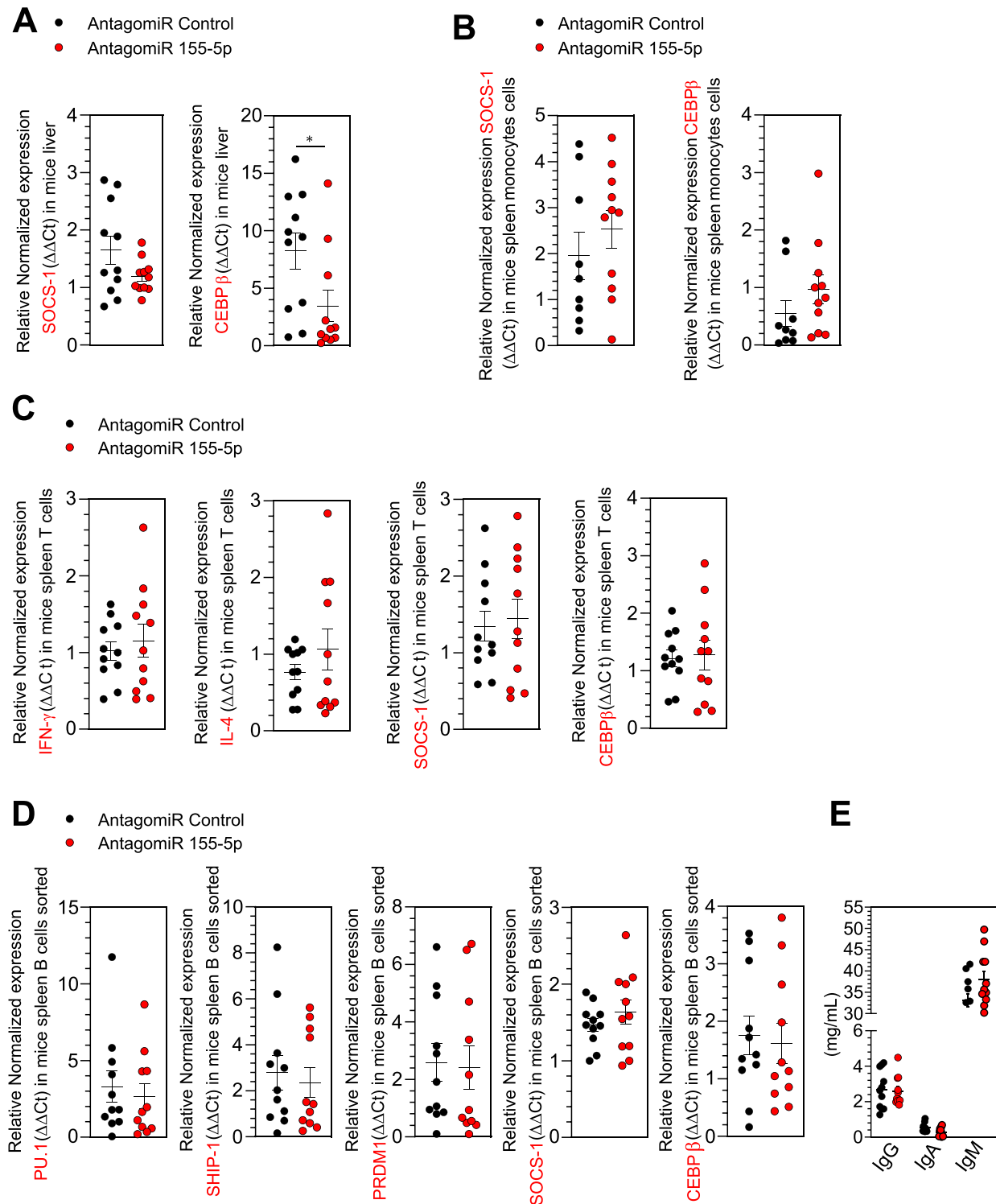


Figure 6. CIA mice treatment in vivo of PEG liposomes containing an antagomiR-155-5p has limited impact on other immune cells. **(A)** qPCR on liver pellets (Kupffer cells) of SOCS-1, CEBP- β , and GAPDH. **(B)** qPCR on sorted spleen monocytes of SOCS-1, CEBP- β , and GAPDH. **(C)** qPCR of spleen of T cells sorted of IFN- γ , IL-4, SOCS-1, CEBP- β , and GAPDH. **(D)** qPCR of spleen sorted B cells of PU.1, SHIP-1, PRDM1, SOCS-1, CEBP- β , and GAPDH. **(E)** ELISA on mice serum for determination of IgG – IgA and IgM. CEBP- β , CCAAT enhancer binding protein β ; GAPDH, glyceraldehyde 3-phosphate dehydrogenase; IFN- γ , interferon γ ; Ig, immunoglobulin; IL-4, interleukin 4; miR, microRNA; PRDM1, PR domain zinc finger protein 1; qPCR, quantitative polymerase chain reaction; SHIP-1, SH2 domain-containing inositol phosphatase 1; SOCS-1, suppressor of cytokine signaling 1.

more important in the high inflammatory STA than in the CIA mice model, and it could be linked to the difference of inflammation between both models. This difference could also be explained by the timing of the analysis in which monocytes were collected for STA near the exponential phase of the disease and/or inflammation, as compared with CIA, in which the monocyte collection was performed on the plateau of the disease and/or inflammation.

PEG liposomes are ideal vectors to improve the addressing of antagomiR to cells for several reasons: (1) they protect antagomiR from enzymatic degradation,¹⁸ (2) they combine the advantages of being biocompatible and nontoxic, and (3) they are predominantly captured by activated phagocytic blood monocytes and macrophages that are present at the site of inflammation. Using targeting ligands could even increase this specificity to monocytes and macrophages. But, until now, no specific receptor of monocytes and macrophages has been established that could increase the delivery in phagocytic monocytes and macrophages. Liposomes also have the advantage of being quickly available and have a good safety profile for clinical translation, as shown by the high number of liposomal drugs on the market. For example, daunorubicin entrapped in liposome has an improved pharmacokinetic profile compared with free daunorubicin, is well tolerated, and had significant antitumor activity in patients with AIDS-related Kaposi's sarcoma.²⁹ Moreover, in 2018, patisiran, a lipid nanoparticle formulation of short interfering RNA for the treatment of hereditary transthyretin-mediated amyloidosis was clinically approved.³⁰ More recently in 2020, SARS-CoV-2 has spread throughout the world and resulted in an unprecedented global public health crisis. In the emergency, six mRNA vaccines have been used to prevent SARS-CoV-2 infection with lipid formulations via intramuscular injection.³¹

The treatment of RA has been markedly improved over the past 20 years with the use of five tumor necrosis factor inhibitors, two IL-6 receptor inhibitors, one costimulation antagonist, one B cell-targeted therapy, and four JAK inhibitors.³² However, none of these treatments target a pathophysiologic pathway specific to RA. Thus, these treatments may lead to some adverse events, as recently illustrated by the increased risk of cancer and of major cardiovascular events with JAK inhibitors compared with tumor necrosis factor inhibitors.³³

Our approach with antagomiR-155-5p encapsulated in PEG liposomes has the advantage of targeting a cellular abnormality, the defect of polarization of monocytes into M2 anti-inflammatory macrophages specific of RA, because we did not find it in other inflammatory diseases.¹¹ In this study, we showed that this defect also exists in two different models of RA. Actually targeting miR-155 could not be specific of monocytes and macrophages. Indeed, several studies proved the involvement and the key role of miR-155 on CD4⁺T cells on activation, differentiation, function, and apoptosis,³⁴ but also on B cells by PU.1 regulation that lead to the survival and proliferation of B blast, plasmablast, and, consequently, antibody production.³⁵ However, thanks to its

encapsulation in liposomes, antagomiR-155-5p had no more of an impact on mRNA targets of miR-155-5p in other immune cells (CD4, CD8, B cells, and plasma cells) than monocytes and macrophages and a limited impact on liver and spleen monocytes and macrophages, thus limiting the possible induction of side effects caused by action on these cells. Indeed, phagocytosis is requested for the availability of the encapsulated antagomiR and is made by monocytes and macrophages. The encapsulated antagomiR-155-5p was present in both cellular types and probably acts at the stage of blood monocytes for reorienting it to a correct differentiation into anti-inflammatory macrophages.

In summary, the encapsulation of antagomiR-155-5p in PEG liposomes appears to be an effective strategy to deliver small RNA to monocytes and macrophages and reduce joint inflammation in mouse models of RA. The repolarization of unbalanced macrophages by PEG liposomes encapsulating antagomiR-155-5p could be a promising, specific, and safe therapeutic strategy to treat human RA.

ACKNOWLEDGMENTS

We are grateful to the staff members of the animal facility in the University of Glasgow, to A. Perrot and S. Mazaudie of the animal facility, University Paris-Saclay and the ANIMEX Chatenay-Malabry for their assistance regarding animal experiment, to C. Bourgeois for assistance regarding cytometry, to D. Vaughan and A. Hamilton of the iii-Flow Core Facility of the University of Glasgow, to F. Apparailly (U1183) for KBxN serum to induce serum transfer arthritis model and to C. Brenner and D. Courilleau, and to the CIBLOT facility at Chatenay-Malabry for efficiency of antagomiR encapsulation in pegylated liposome.

AUTHOR CONTRIBUTIONS

All authors were involved in drafting the article or revising it critically for important intellectual content, and all authors approved the final version to be published. Dr. Paoletti had full access to all of the data in the study and takes responsibility for the integrity of the data and the accuracy of the data analysis.

Study conception and design. Paoletti, Reboud, Fay, Nocturne, Tsapis, McInnes, Kurowska-Stolarska, Fattal, Mariette.

Acquisition of data. Paoletti, Ly, Cailleau, Gao.

Analysis and interpretation of data. Paoletti, Ly, Cailleau, Gao, Mariette.

REFERENCES

- McInnes IB, Schett G. Pathogenetic insights from the treatment of rheumatoid arthritis. *Lancet* 2017;389(10086):2328–2337.
- Bresnihan B, Pontifex E, Thurlings RM, et al. Synovial tissue sublining CD68 expression is a biomarker of therapeutic response in rheumatoid arthritis clinical trials: consistency across centers. *J Rheumatol* 2009;36(8):1800–1802.
- Kawanaka N, Yamamura M, Aita T, et al. CD14⁺, CD16⁺ blood monocytes and joint inflammation in rheumatoid arthritis. *Arthritis Rheum* 2002;46(10):2578–2586.
- Degboé Y, Poupot R, Poupot M. Repolarization of unbalanced macrophages: unmet medical need in chronic inflammation and cancer. *Int J Mol Sci* 2022;23(3):1496.

5. Alivernini S, MacDonald L, Elmesmari A, et al. Distinct synovial tissue macrophage subsets regulate inflammation and remission in rheumatoid arthritis. *Nat Med* 2020;26(8):1295–1306.
6. Shoda J, Tanaka S, Etori K, et al. Semaphorin 3G exacerbates joint inflammation through the accumulation and proliferation of macrophages in the synovium. *Arthritis Res Ther* 2022;24(1):134.
7. Huang QQ, Doyle R, Chen SY, et al. Critical role of synovial tissue-resident macrophage niche in joint homeostasis and suppression of chronic inflammation. *Sci Adv* 2021;7(2):eabd0515.
8. Elmesmari A, Fraser AR, Wood C, et al. MicroRNA-155 regulates monocyte chemokine and chemokine receptor expression in rheumatoid arthritis. *Rheumatology (Oxford)* 2016;55(11):2056–2065.
9. Stanczyk J, Pedrioli DM, Brentano F, et al. Altered expression of MicroRNA in synovial fibroblasts and synovial tissue in rheumatoid arthritis. *Arthritis Rheum* 2008;58(4):1001–1009.
10. Paoletti A, Rohmer J, Ly B, et al. Monocyte/macrophage abnormalities specific to rheumatoid arthritis are linked to miR-155 and are differentially modulated by different TNF inhibitors. *J Immunol* 2019;203(7):1766–1775.
11. Kurowska-Stolarska M, Alivernini S. Synovial tissue macrophages in joint homeostasis, rheumatoid arthritis and disease remission. *Nat Rev Rheumatol* 2022;18(7):384–397.
12. Kurowska-Stolarska M, Alivernini S, Ballantine LE, et al. MicroRNA-155 as a proinflammatory regulator in clinical and experimental arthritis. *Proc Natl Acad Sci USA* 2011;108(27):11193–11198.
13. Caplazi P, Baca M, Barck K, et al. Mouse models of rheumatoid arthritis. *Vet Pathol* 2015;52(5):819–826.
14. Kollias G, Papadaki P, Apparailly F, et al. Animal models for arthritis: innovative tools for prevention and treatment. *Ann Rheum Dis* 2011;70(8):1357–1362.
15. Christensen AD, Haase C, Cook AD, et al. K/BxN serum-transfer arthritis as a model for human inflammatory arthritis. *Front Immunol* 2016;7:213.
16. Alivernini S, Gremese E, McSharry C, et al. MicroRNA-155 at the critical interface of innate and adaptive immunity in arthritis. *Front Immunol* 2018;8:1932.
17. Lorscheider M, Tsapis N, Ur-Rehman M, et al. Dexamethasone palmitate nanoparticles: an efficient treatment for rheumatoid arthritis. *J Control Release* 2019;296:179–189.
18. Fattal E, Fay F. Nanomedicine-based delivery strategies for nucleic acid gene inhibitors in inflammatory diseases. *Adv Drug Deliv Rev* 2021;175:113809.
19. Rice J, Roberts H, Rai SN, Galandiuk S. Housekeeping genes for studies of plasma microRNA: a need for more precise standardization. *Surgery* 2015;158(5):1345–1351.
20. Gawne PJ, Clarke F, Turjeman K, et al. PET imaging of liposomal glucocorticoids using ⁸⁹Zr-oxine: theranostic applications in inflammatory arthritis. *Theranostics* 2020;10(9):3867–3879.
21. Goel H, Siddiqui L, Mahtab A, et al. Chapter 2 - Fabrication design, process technologies, and convolutions in the scale-up of nanotherapeutic delivery systems. In: Kesharwani P, Singh KK, eds. *Nanoparticle Therapeutics: Production Technologies, Types of Nanoparticles, and Regulatory Aspects*. Elsevier; 2021:47–131.
22. Kamps JAAM, Scherphof GL. 16 - Biodistribution and uptake of liposomes in vivo. *Methods Enzymol* 2004;387:257–266.
23. Rahman M, Alam K, Beg S, Anwar F, Kumar V. Chapter 6 - Liposomes as topical drug delivery systems: state of the arts. In: Grumezescu AM, ed. *Biomedical Applications of Nanoparticles*. Elsevier; 2019:149–161.
24. Rana AK, Li Y, Dang Q, Yang F. Monocytes in rheumatoid arthritis: circulating precursors of macrophages and osteoclasts and, their heterogeneity and plasticity role in RA pathogenesis. *Int Immunopharmacol* 2018;65:348–359.
25. Yano R, Yamamura M, Sunahori K, et al. Recruitment of CD16+ monocytes into synovial tissues is mediated by fractalkine and CX3CR1 in rheumatoid arthritis patients. *Acta Med Okayama* 2007;61(2):89–98.
26. Culemann S, Grüneboom A, Nicolás-Ávila JÁ, et al. Locally renewing resident synovial macrophages provide a protective barrier for the joint. *Nature* 2019;572(7771):670–675.
27. Blüml S, Bonelli M, Niederreiter B, et al. Essential role of microRNA-155 in the pathogenesis of autoimmune arthritis in mice. *Arthritis Rheum* 2011;63(5):1281–1288.
28. Caplazi P, Baca M, Barck K, et al. Mouse models of rheumatoid arthritis. *Vet Pathol* 2015;52(5):819–826.
29. Gill PS, Espina BM, Muggia F, et al. Phase I/II clinical and pharmacokinetic evaluation of liposomal daunorubicin. *J Clin Oncol* 1995;13(4):996–1003.
30. Zhang X, Goel V, Attarwala H, et al. Patisiran pharmacokinetics, pharmacodynamics, and exposure-response analyses in the phase 3 APOLLO trial in patients with hereditary transthyretin-mediated (hATTR) amyloidosis. *J Clin Pharmacol* 2020;60(1):37–49.
31. Dong Y, Dai T, Wei Y, et al. A systematic review of SARS-CoV-2 vaccine candidates. *Signal Transduct Target Ther* 2020;5(1):237.
32. Burmester GR, Pope JE. Novel treatment strategies in rheumatoid arthritis. *Lancet* 2017;389(10086):2338–2348.
33. Ytterberg SR, Bhatt DL, Mikuls TR, et al; ORAL Surveillance Investigators. Cardiovascular and cancer risk with tofacitinib in rheumatoid arthritis. *N Engl J Med* 2022;386(4):316–326.
34. Chen L, Gao D, Shao Z, et al. miR-155 indicates the fate of CD4⁺ T cells. *Immunol Lett* 2020;224:40–49.
35. Arbore G, Henley T, Biggins L, et al. MicroRNA-155 is essential for the optimal proliferation and survival of plasmablast B cells. *Life Sci Alliance* 2019;2(3):e201800244.